#46

Papers from the GEOPHYSICAL LABORATORY
Carnegie Institution of Washington
VOL. 84, NO. B12 JOURNAL OF GEOPHYSICAL RESEARCH No. 1787 NOVEMBER 10, 1979

Bulk Modulus–Volume Relationship for Cation-Anion Polyhedra

ROBERT M. HAZEN AND LARRY W. FINGER

Geophysical Laboratory, Carnegie Institution of Washington, Washington, D.C. 20008

A bulk modulus–volume relationship is demonstrated for cation coordination polyhedra in a variety of structure types including oxides, silicates, halides, sulfides, phosphides, and carbides: $K_p \langle d \rangle^3 / S^2 z_c z_a = 7.5$ (Mbar Å^3), where K_p is the polyhedral bulk modulus (in megabars), $\langle d \rangle$ is the mean cation-anion separation (in angstroms), z_c and z_a are the cation and anion formal charge, and S^2 is an empirical ionicity term, defined as 0.50 for oxides and silicates and calculated to be 0.75 for halides; 0.40 for sulfides, selenides, and tellurides; 0.25 for phosphides, arsenides, and antimonides; and 0.20 for carbides. The bulk modulus of a substance depends on the bulk moduli of component polyhedra and the manner in which these polyhedra are linked. In corner-linked structures, such as quartz and framework silicates, mineral bulk moduli are significantly less than those of constituent corner-linked polyhedra, because of accommodations resulting from changes of the metal-oxygen-metal angles. In layer structures such as micas, with extensive edge sharing within the layers but weak bonds between the layers, compression is highly anisotropic. Structures such as periclase, spinel, and garnet, with extensive edge sharing between polyhedra in three dimensions, have large bulk moduli similar to those of constituent polyhedra. Bulk moduli of mantle mineral phases approximate the moduli of component polyhedra because most mantle mineral structure types have edge sharing in three dimensions. Compression for a given polyhedron does not appear to depend upon the linkage topology of the structure.

INTRODUCTION

Empirical relationships between bulk modulus and molar volume were first proposed by *Bridgman* [1923] and have subsequently developed into important tools for predicting physical properties of minerals [*Anderson and Nafe*, 1965; *Anderson and Anderson*, 1970; *Anderson*, 1972]. Theoretical arguments for such relationships, based on a simple two-term model of atomic bonding, may also be applied to subunits of a crystal structure, for example, cation coordination polyhedra or cation-anion bonds. Recent advances in high-pressure, single-crystal X ray crystallography have enabled the researcher to measure structural parameters such as bond distances in complex crystals as a function of pressure. Hence bulk modulus–volume systematics may now be tested for polyhedral elements of oxides and silicates. The resulting relationships yield information about the geometry of mineral compression and provide constraints on the nature of the repulsive energy parameter of bonding.

CRYSTAL STRUCTURE DATA

Empirical bulk modulus–volume relationships for cation-anion coordination groups may be derived from two types of data, as presented in Table 1. Many simple compounds, including those with NaCl and CaF_2 structures, have cation-anion separations that are simply related to molar volume. For these materials, data in Table 1 are easily calculated from the bulk modulus and molar volume of the compound. The other data in Table 1 are derived from high-pressure X ray diffraction experiments on single crystals, from which atomic positions (and, consequently, bond distances and compressibilities) are determined as a function of pressure.

If we consider only the 38 polyhedra from oxides and silicates (Table 1), a relationship analogous to that proposed by *Hazen and Prewitt* [1977*a*] is obtained:

$$K_p \langle d \rangle^3 / z_c = 7.5 \pm 0.2 \text{ Mbar Å}^3 \quad (1)$$

where K_p is the polyhedral bulk modulus (in megabars), $\langle d \rangle$ is the mean cation-anion separation (in angstroms), and z_c is the cation formal charge. Polyhedral bulk moduli may be calculated directly from polyhedral volume data as determined from X ray structure analysis or from linear compressibilities of cation-anion bonds. If $\langle \beta \rangle$ is the mean linear compressibility of a group of cation-anion bonds, then an 'effective polyhedral bulk modulus' may be defined as

$$K_p = 1/3\langle \beta \rangle$$

If we use this relationship, (1) may be applied to planar and linear, as well as polyhedral, cation coordination groups. Polyhedral data used to derive (1) are illustrated in Figure 1. The coefficient in (1) was calculated from weighted linear regression of data in Table 1 and was constrained to pass through the origin. Calculations were performed using both K_p^{-1} and $\langle d \rangle^3 / z_c$ as independent variables; 7.5 ± 0.2 is the average coefficient. Weighted regression of K_p versus $z_c / \langle d \rangle^3$ yields a slightly smaller coefficient of 7.3 ± 0.2. Bulk moduli from fully constrained structures, notably NaCl-type oxides, are known more precisely than other polyhedral bulk moduli; the coefficient is therefore heavily weighted by these oxides. Almost all data, however, lie within two estimated standard deviations of the predicted bulk moduli.

A similar bulk modulus–volume relationship for halides may also be derived:

$$K_p \langle d \rangle^3 / z_c = 5.6 \pm 0.1 \text{ Mbar Å}^3 \quad (2)$$

Equation (1) for oxides and (2) for halides may be combined with other data on sulfides, selenides, tellurides, phosphides, arsenides, antimonides, and carbides into a more general bulk modulus–volume relationship:

$$K_p \langle d \rangle^3 / S^2 z_c z_a = 7.5 \pm 0.2 \text{ Mbar Å}^3 \quad (3)$$

where z_a is the anion formal charge and S^2 is an empirical term for the relative 'ionicity' of the bond, defined as 0.50 for R^{2+} –O bonds in NaCl-type oxides. Equation (3) is similar in form to (5) of *Anderson* [1972, p. 278], which is valid for the bulk properties of several simple compounds. When applied to bulk mineral properties, however, the constant may vary, depending on structure type. Furthermore, the appropriate value of $z_c z_a$ in many complex compounds is not obvious. In

Paper number 9B1030.
0148-0227/79/009B-1030$01.00

TABLE 1. Polyhedral Bulk Moduli, Bond Distances, and Bonding Parameters for a Variety of Compounds

Compound (Polyhedron)	Structure Type	$\langle d \rangle$,[1] Å	K_p,[2] Mbar	z_c	z_a	S^2	$\frac{K_p \langle d \rangle^3}{S^2 z_c z_a}$	Reference[3]
NiO	NaCl[4]	2.084	1.96 (10)	2	2	0.50	8.9	1
MgO	NaCl[4]	2.106	1.61 (5)	2	2	0.50	7.5	2
CoO	NaCl[4]	2.133	1.85 (9)	2	2	0.50	9.0	1
FeO	NaCl[4]	2.139	1.53 (8)	2	2	0.50	7.5	3
MnO	NaCl[4]	2.222	1.43 (7)	2	2	0.50	7.8	1
CaO	NaCl[4]	2.406	1.10 (5)	2	2	0.50	7.7	1
SrO	NaCl[4]	2.580	0.91 (5)	2	2	0.50	7.8	4
BaO	NaCl[4]	2.776	0.69 (4)	2	2	0.50	7.4	5
BeO	zincite	1.66	2.5 (5)	2	2	0.50	5.7	6
ZnO	zincite	1.80	1.4 (3)	2	2	0.50	4.2	6
UO_2	fluorite[4]	2.37	2.3 (1)	4	2	0.50	7.7	7
ThO_2	fluorite[4]	2.42	1.93 (10)	4	2	0.50	6.8	6
Al_2O_3	corundum	1.91	2.4 (2)	3	2	0.50	5.6	8
Fe_2O_3	corundum	1.98	2.3 (3)	3	2	0.50	6.0	8
Cr_2O_3	corundum	1.99	2.3 (3)	3	2	0.50	6.1	8
V_2O_3	corundum	2.01	1.8 (3)	3	2	0.50	4.9	8
SiO_2	rutile[5]	1.778	3.2 (1.5)	4	2	0.50	4.4	9
GeO_2	rutile	1.884	2.7 (1.0)	4	2	0.50	4.4	7
TiO_2	rutile	1.961	2.2 (1.0)	4	2	0.50	4.2	7
RuO_2	rutile	1.968	2.7 (1.0)	4	2	0.50	5.1	7
MnO_2	rutile[5]	1.88	2.8 (1.0)	4	2	0.50	4.7	9
SnO_2	rutile	2.054	2.3 (1.0)	4	2	0.50	5.2	7
SiO_2	quartz[6]	1.61	>5	4	2	0.50	>5.3	10
GeO_2	quartz[6]	1.73	>4	4	2	0.50	>5.2	10
Pyrope (Mg-O)	garnet	2.27	1.3 (1)	2	2	0.50	7.6	11
Pyrope (Al-O)	garnet	1.89	2.2 (5)	3	2	0.50	5.0	11
Pyrope (Si-O)	garnet	1.63	3 (1)	4	2	0.50	3.2	11
Grossular (Ca-O)	garnet	2.40	1.15 (13)	2	2	0.50	7.9	11
Grossular (Al-O)	garnet	1.93	2.2 (5)	3	2	0.50	5.3	11
Grossular (SiO)	garnet	1.64	3 (1)	4	2	0.50	3.3	11
Forsterite (Mg-O)	olivine	2.12	1.5 (3)	2	2	0.50	7.0	12
γ Ni_2SiO_4 (Ni-O)	spinel	2.06	1.5 (3)	2	2	0.50	6.6	13
γ Ni_2SiO_4 (Si-O)	spinel[6]	1.66	>2.5	4	2	0.50	>2.9	13
Fassaite (Ca-O)	clinopyroxene	2.49	0.85 (20)	2	2	0.50	6.6	14
Phlogopite (K-O)	mica	2.97	0.27 (6)	1	2	0.50	7.1	15
Albite (Na-O)	feldspar	2.75	0.32 (6)	1	2	0.50	6.7	16
Zircon (Zr-O)	zircon	2.20	2.8 (3)	4	2	0.50	7.5	17
Zircon (Si-O)	zircon[6]	1.61	>2.5	4	2	0.50	>2.6	17
LiF	NaCl[4]	2.023	0.66 (3)	1	1	0.75	7.3	18
NaF	NaCl[4]	2.310	0.45 (2)	1	1	0.75	7.4	18
KF	NaCl[4]	2.674	0.293 (15)	1	1	0.75	7.5	18
RbF	NaCl[4]	2.820	0.273 (14)	1	1	0.75	8.2	6
LiCl	NaCl[4]	2.565	0.315 (16)	1	1	0.75	7.0	6
NaCl	NaCl[4]	2.814	0.240 (12)	1	1	0.75	7.1	6
KCl	NaCl[4]	3.146	0.180 (9)	1	1	0.75	7.5	6
RbCl	NaCl[4]	3.291	0.160 (8)	1	1	0.75	7.6	6
LiBr	NaCl[4]	2.750	0.257 (13)	1	1	0.75	7.1	6
NaBr	NaCl[4]	2.989	0.200 (10)	1	1	0.75	7.1	6
KBr	NaCl[4]	3.264	0.152 (8)	1	1	0.75	7.0	6
RbBr	NaCl[4]	3.427	0.138 (7)	1	1	0.75	7.4	6
LiI	NaCl[4]	3.000	0.188 (9)	1	1	0.75	6.8	6
NaI	NaCl[4]	3.236	0.161 (8)	1	1	0.75	7.3	6
KI	NaCl[4]	3.533	0.124 (6)	1	1	0.75	7.3	6
RbI	NaCl[4]	3.671	0.111 (6)	1	1	0.75	7.3	6
CsCl	CsCl[4]	3.57	0.182 (9)	1	1	0.75	11.1	18
CsBr	CsCl[4]	3.71	0.155 (8)	1	1	0.75	10.6	6
CsI	CsCl[4]	3.95	0.129 (6)	1	1	0.75	10.6	6
ThCl	CsCl[4]	3.32	0.236 (12)	1	1	0.75	11.5	6
ThBr	CsCl[4]	3.43	0.225 (11)	1	1	0.75	12.0	6
CuCl	cubic ZnS[4]	2.34	0.40 (2)	1	1	0.75	6.8	6
AgI	cubic ZnS[4]	2.80	0.243 (12)	1	1	0.75	7.1	3
CaF_2	fluorite[4]	2.36	0.86 (4)	2	1	0.75	7.6	6
BaF_2	fluorite[4]	2.68	0.57 (3)	2	1	0.75	7.3	6
PbF_2	fluorite[4]	2.57	0.61 (3)	2	1	0.75	6.9	6
SrF_2	fluorite[4]	2.51	0.70 (4)	2	1	0.75	7.4	6
MgF_2	rutile[5]	1.99	1.0 (3)	2	1	0.75	5.3	6
MnF_2	rutile	2.12	0.9 (2)	2	1	0.75	5.7	19
TaC	NaCl[4]	2.227	2.2 (2)	4	4	0.2	7.6	6
TiC	NaCl[4]	2.159	1.9 (2)	4	4	0.2	6.0	6
UC	NaCl[4]	2.480	1.6 (1)	4	4	0.2	7.6	6
ZrC	NaCl[4]	2.341	1.9 (2)	4	4	0.2	7.6	6

TABLE 1. (continued)

Compound (Polyhedron)	Structure Type	$\langle d \rangle$,[1] Å	K_p,[2] Mbar	z_c	z_a	S^2	$\frac{K_p \langle d \rangle^3}{S^2 z_c z_a}$	Reference[3]
C	diamond[4]	1.544	5.8 (3)	4	4	0.2	6.7	6
C (planar C-C)	graphite[7]	1.42	5.9 (3)	4	4	0.2	5.3	20
CaS	NaCl[4]	2.845	0.43 (2)	2	2	0.4	6.2	3
SrS	NaCl[4]	3.010	0.40 (2)	2	2	0.4	6.8	3
BaS	NaCl[4]	3.194	0.35 (2)	2	2	0.4	7.2	3
PbS	NaCl[4]	2.968	0.48 (3)	2	2	0.4	7.8	3
CdS	zincite	2.43	0.61 (6)	2	2	0.4	5.5	6
ZnS	zincite	2.24	0.77 (8)	2	2	0.4	5.4	6
ZnS	cubic ZnS[4]	2.34	0.76 (4)	2	2	0.4	6.1	6
SnS_2	CdI_2	2.56	1.2 (2)	4	2	0.4	6.3	15
ZnSe	cubic ZnS[4]	2.45	0.60 (3)	2	2	0.4	5.5	6
CaSe	NaCl[4]	2.960	0.49 (2)	2	2	0.4	7.9	3
SrSe	NaCl[4]	3.115	0.43 (2)	2	2	0.4	8.1	3
BaSe	NaCl[4]	3.300	0.36 (2)	2	2	0.4	8.1	3
PbSe	NaCl[4]	3.062	0.34 (2)	2	2	0.4	6.1	3
CdSe	zincite	2.35	0.54 (5)	2	2	0.4	4.4	6
CaTe	NaCl[4]	3.178	0.42 (2)	2	2	0.4	8.4	3
SrTe	NaCl[4]	3.235	0.334 (16)	2	2	0.4	7.1	3
BaTe	NaCl[4]	3.493	0.305 (15)	2	2	0.4	8.1	3
PbTe	NaCl[4]	3.227	0.41 (2)	2	2	0.4	8.6	6
SnTe	NaCl[4]	3.157	0.42 (2)	2	2	0.4	8.4	6
CdTe	cubic ZnS[4]	2.81	0.42 (2)	2	2	0.4	5.9	6
HgTe	cubic ZnS[4]	2.78	0.44 (2)	2	2	0.4	5.9	6
ZnTe	cubic ZnS[4]	2.64	0.51 (3)	2	2	0.4	5.9	6
GaSb	NaCl[4]	3.059	0.56 (3)	3	3	0.25	7.1	6
InSb	NaCl[4]	3.239	0.47 (2)	3	3	0.25	7.1	6
GaAs	NaCl[4]	2.827	0.75 (4)	3	3	0.25	7.5	6
InAs	NaCl[4]	3.018	0.58 (3)	3	3	0.25	7.1	6
GaP	NaCl[4]	2.736	0.89 (4)	3	3	0.25	8.0	6
InP	NaCl[4]	2.934	0.73 (4)	3	3	0.25	8.1	6
BN (linear B-N)	boron nitride[7]	1.45	4.4 (2)	3	3	0.2	7.5	20
KCN	NaCl[4]	3.263	0.143 (7)	1	1	0.75	6.6	6

[1]Error in bond distances at room pressure are ≤0.005 Å.

[2] Error in polyhedral bulk moduli are assumed to be ±5% for fully constrained structures, unless worse precision is reported. Errors in polyhedral bulk moduli of unconstrained structures are generally greater than ±10%.

[3]References are 1, *Clendenen and Drickamer* [1966]; 2 *Schreiber and Anderson* [1966]; 3, *Birch* [1966]; 4, *Liu and Bassett* [1973]; 5 *Liu and Bassett* [1972]; 6 *Simmons and Wang* [1971]; 7 *Hazen and Finger* [1979*b*]; 8 *Sato and Akimoto* [1979] and *Finger and Hazen* [1977]; 9, *Bassett and Takahashi* [1974]; 10 *Jorgensen* [1978]; 11, *Hazen and Finger* [1978*b*]; 12, *Hazen* [1976]; 13, *Finger et al.* [1979]; 14, *Hazen and Finger* [1977]; 15, *Hazen and Finger* [1978*c*]; 16, *Hazen and Prewitt* [1977*b*]; 17 *Hazen and Finger* [1979*c*]; 18, *Yagi* [1978]; 19, *Hazen et al.* [1978]; 20, *Lynch and Drickamer* [1966].

[4]Fully constrained structure in which the polyhedral bulk modulus is identical to the crystal bulk modulus.

[5]High-pressure crystal structures of rutile-type SiO_2, MnO_2, and MgF_2 have not been done. Studies of other rutile-type compounds (references 7 and 19) indicate that polyhedral bulk moduli agree within ±30% of crystal bulk moduli.

[6]Tetrahedral bulk moduli of these compounds are greater than the indicated value. No upper limit is reported because net compression of the bond is comparable to the standard error of the bond distance.

[7]In graphite and boron nitride, bond compression is constrained to be equal to unit cell compression within the (001) plane.

$NaNO_2$, for example, bulk modulus–volume data fit the alkali halide trend with $z_c z_a = 1$; this value does not apply to $NaNO_3$, however [*Hazen and Finger*, 1979*a*]. These difficulties are not present when (3) is applied to cation coordination groups. A single constant appears to fit many different structure types, and the values of z_c and z_a are unambiguous.

Values of S^2 may be calculated from equations such as (1) and (2) for each type of anion. (Until a better measure of ionicity is available, it will be assumed that S^2 is constant for a given anion.) If S^2 is defined to be 0.50 for all oxides and silicates, then combining (2) and (3) yields S^2 for halides of ≈0.75. Empirical values of S^2 determined in this way for other anions are 0.40 for sulfides, selenides, and tellurides; 0.25 for phosphides, arsenides, and antimonides; and 0.20 for carbides. Of the oxide and silicate polyhedra used to construct Figure 1 those that deviate most from the empirical line are tetrahedra, such as Si in silicates and Zn in ZnO, and octahedrally coordinated vanadium in V_2O_3, an unusual oxide with metallic luster and conductivity. All these polyhedra, which are more compressible than indicated by (3), also have bonding that is more covalent than in the other plotted oxide and silicate polyhedra (i.e., S^2 may be less than 0.50). Thus deviations from the line in Figure 1 may provide an approximate measure of ionicity.

Figure 2 illustrates (3) for polyhedra in more than 100 substances in 19 different structure types from data in Table 1. It is significant that a simple empirical relationship successfully models bond compression in materials with a wide range of bond character and topology. Of the structures examined, only CsCl is anomalous with all points falling significantly below the empirical line (Figure 2). This structure, with eight anions at the corners of each unit cube and a cation at the cube's center, is unique in the high degree of face sharing between adjacent polyhedra and the consequent short cation-cation separations. In CsCl-type compounds the cation-cation separation is only 15% longer than cation-anion bonds, in contrast to the 50–100% greater separation in most other structures. It is probable therefore that (3), which considers only the primary coordination group of a cation, is not valid for structures (for example, perovskite?) in which extensive

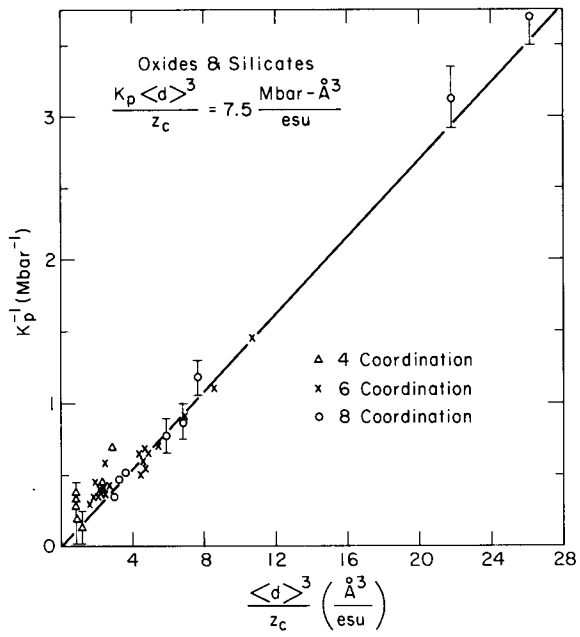

Fig. 1. The bulk modulus–volume relationship for polyhedra in oxides and silicates. Triangles represent tetrahedra, crosses octahedra, and circles eight or greater coordination. Error bars represent one estimated standard deviation in polyhedral bulk moduli for selected polyhedra in silicates. The line is a weighted linear regression fit of all data, constrained to pass through the origin. This line is largely determined by polyhedra in fixed-structure oxides for which polyhedral bulk-modulus errors are small. Almost all points, however, lie within two estimated standard deviations of predicted bulk moduli.

face sharing results in strong second-nearest neighbor interactions.

Relationships Between Crystal Structure and Compression

An important consequence of (3) is that in most structures, polyhedral bulk moduli are independent of polyhedral linkages. Polyhedra in a crystal therefore are not analogous to mineral grains in a rock, which may experience differing degrees of compression depending on the geometry and strength of surrounding grains. In most mineral structures each polyhedron is subjected to the full external pressure (although anisotropic compression, of course, may result).

In all but a few simple structure types, polyhedral bulk moduli are not simply related to macroscopic bulk moduli; polyhedral linkages must also be considered. Two cation polyhedra may be linked by a shared face, a shared edge, a shared corner, or Van der Waal's forces. The type and distribution of these polyhedral linkages are the most important factors in determining the bulk modulus of a compound. All oxides and silicates have a bulk modulus that is less than or equal to that of the least compressible polyhedron. The degree to which mineral bulk moduli differ from polyhedral bulk moduli depends on the rigidity of polyhedral linkages.

The most rigid polyhedral linkage is one in which polyhedra share faces or edges in three dimensions. If each shared edge between polyhedra is represented as a line segment in space, then all such line segments may form a continuous three-dimensional array. In these fully edge-linked structures (including halite, corundum, spinels, and garnets) any change in molar volume must be accompanied by a change in metal-oxygen bond distances because of the rigid polyhedral linkages. Bulk moduli of these materials, consequently, are large because they are similar in magnitude to bulk moduli of metal-oxygen polyhedra. In periclase and corundum, for example, bulk moduli of the octahedral sites, the only polyhedra, and the bulk mineral are identical. In silicate spinels and garnets, having both silicate tetrahedra and larger divalent cation polyhedra, the mineral bulk moduli are intermediate between the polyhedral bulk moduli of these Si^{4+} and R^{2+} sites.

In contrast to the materials described above, some structures such as α quartz, feldspar, and zeolites have primarily corner-linked polyhedra. In these framework structures, volume changes may be effected by changes in angles between tetrahedra, without altering T-O distances. Framework silicates, consequently, have relatively small bulk moduli, even though individual tetrahedral polyhedra undergo small volume changes with pressure. The tilting of polyhedra in compression of corner-linked materials may be treated as primarily metal-oxygen-metal bond bending or oxygen-oxygen compression, as opposed to metal-oxygen compression. It should be noted, however, that bulk moduli of feldspars and many zeolites are closely related to the bulk moduli of large alkali cation polyhedra. If alkali sites are assumed to share edges with the (Al, Si) tetrahedra, then feldspars and zeolites may be treated as fully linked by shared edges, and mineral bulk moduli should be closely approximated by volume changes of the large cation sites.

In most structures, including pyroxenes, olivines, and rutile-type compounds, all polyhedra share edges with some adjacent polyhedra and link corners with others; a continuous three-dimensional edge linkage does not obtain. In these materials, compression is due to a combination of polyhedral (metal-oxygen) compression and oxygen-oxygen compression, and the net volume change may be greater than that of component polyhedra. The significant differences between poly-

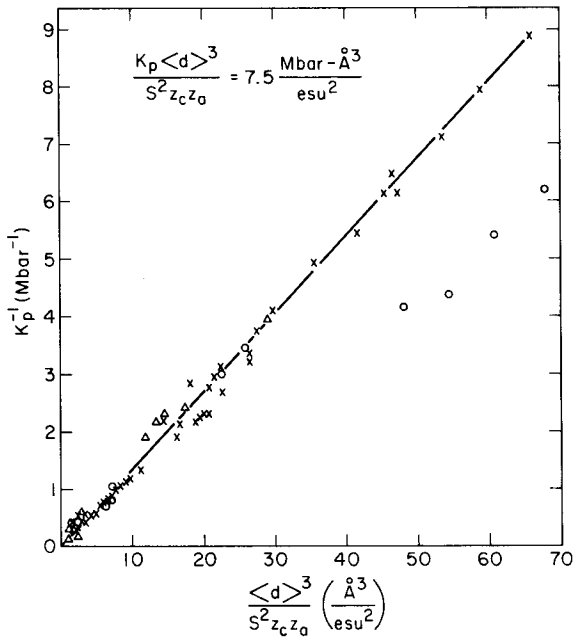

Fig. 2. The bulk modulus–volume relationship for polyhedra in a variety of materials. Triangles, crosses, and circles indicate coordination as in Figure 1.

hedral linkages of olivines and silicate spinels, for example, lead to the much smaller bulk moduli of the former.

The effect of linkage rigidity on mineral compression is dramatically illustrated by layer minerals. In materials such as brucite, talc, and chlorite, weak interlayer Van der Waal's bonds lead to linear compressibilities between layers many times greater than within layers [*Hazen and Finger, 1978a*]. Phlogopite mica, $KMg_3AlSi_3O_{10}(OH)_2$, has fully linked edge-sharing magnesium octahedra in two dimensions within layers but weak K-O bonds between layers. The intralayer linear compressibility (2.2×10^{-4} kbar^{-1}) is identical with that of periclase, MgO, which is fully linked in three dimensions. The interlayer linear compression of phlogopite, however, is more than 5 times greater, owing to the large compressibility of the K-O bonds.

Anisotropic compression of many other minerals is also due in large part to nonuniform distribution of polyhedral linkages. In rutile-type compounds, for example, close approach of metal cations across shared edges leads to the low compressibility of c relative to a [*Hazen et al., 1978*]. There is thus a close relationship between the type and distribution of polyhedral linkages and the bulk moduli of oxygen-based compounds.

PREDICTION OF MACROSCOPIC BULK MODULI

Compression of oxygen-based compounds is due to both polyhedral compression, which appears to be a fundamental property independent of structure, and polyhedral tilting, which is dependent on the structural linkages of polyhedra. In order to predict the bulk modulus of a compound it is necessary to know the bulk moduli of the component polyhedra and the nature of the polyhedral linkages. For many crustal minerals, linkages are complex, and accurate prediction of bulk moduli is not yet possible. (Recent measurements of metal-oxygen-metal bending force constants may lead to predictions of polyhedral tilting magnitudes (G. V. Gibbs, personal communications, 1978).) On the other hand, dense oxide and silicate phases that are predicted to exist in the transition zone and lower mantle have full three-dimensional edge sharing. Prediction of the bulk moduli of these mantle phases, even if details of atomic arrangements are unknown, may thus be greatly simplified.

CONCLUSIONS

The bulk modulus–volume relationship for cation coordination polyhedra is a useful empirical equation for predicting the geometry of compression in many solids. The relationship may also be used to predict approximate macroscopic bulk moduli in some fully linked structures, although uncertainties in the magnitudes of polyhedral tilting and in the ionicity coefficients of different bonds limit this application. Equation (3) therefore is not intended as a substitute for the successful bulk modulus–volume relationships of *Anderson* [1972] and others.

Equation (3) places important constraints on theoretical models of compression and bonding [see *Anderson,* 1972, equation (3)], although this relationship is not itself an explanation of cation-anion compression. The empirical bulk modulus–volume relationship for polyhedra therefore should be considered in the formulation of models of interatomic forces, as well as in the description and prediction of mineral compression.

Acknowledgments. The authors gratefully acknowledge the contributions of Charles T. Prewitt, whose ideas, discussions, and constructive review of the manuscript are reflected throughout this work. Important concepts and modifications were suggested by L. C. Allen, P. M. Bell, I. D. Brown, M. S. T. Bukowinski, G. V. Gibbs, R. Jeanloz, H. E. King, R. C. Liebermann, H. K. Mao, T. Yagi, and H. S. Yoder, Jr. The work was sponsored in part by National Science Foundation grant EAR77-23171.

REFERENCES

Anderson, D. L., and O. L. Anderson, The bulk modulus–volume relationship for oxides, *J. Geophys. Res., 75,* 3494–3500, 1970.

Anderson, O. L., Patterns in elastic constants of minerals important to geophysics, in *Nature of the Solid Earth,* edited by E. C. Robertson, pp. 575–613, McGraw-Hill, New York, 1972.

Anderson, O. L., and J. E. Nafe, The bulk modulus–volume relationship for oxide compounds and related geophysical problems, *J. Geophys. Res., 70,* 3951–3963, 1965.

Bassett, W. A., and T. Takahashi, X ray diffraction studies up to 300 kbar, *Advan. High Pressure Res., 4,* 165–247, 1974.

Birch, F., Compressibility: Elastic constants, Handbook of Physical Constants, *Geol. Soc. Amer. Mem., 97,* 97–173, 1966.

Bridgman, P. W., The compressibility of thirty metals as a function of pressure and temperature, *Proc. Amer. Acad. Arts Sci., 58,* 165–242, 1923.

Clendenen, R. L., and H. G. Drickamer, Lattice parameters of nine oxides and sulfides as a function of pressure, *J. Chem. Phys., 44,* 4223–4228, 1966.

Finger, L. W., and R. M. Hazen, Bulk moduli and high-pressure crystal structures of Fe_2O_3 and V_2O_3: A comparison with Al_2O_3 and Cr_2O_3 (abstract), *Eos Trans. AGU, 60,* 386, 1979.

Finger, L. W., R. M. Hazen, and T. Yagi, Crystal structure and electron densities of nickel and iron silicate spinels at elevated temperature or pressure, *Amer. Mineral., 62,* in press, 1979.

Hazen, R. M., Effects of temperature and pressure on the crystal structure of forsterite, *Amer. Mineral., 61,* 1280–1293, 1976.

Hazen, R. M., and L. W. Finger, Compressibility and crystal structure of Angra dos Reis fassaite to 52 kbar, *Carnegie Inst. Wash. Yearb., 76,* 512–515, 1977.

Hazen, R. M., and L. W. Finger, Crystal structures and compressibilities of layer minerals at high pressure, II, Phlogopite and chlorite, *Amer Mineral., 63,* 293–296, 1978*a*.

Hazen, R. M., and L. W. Finger, Crystal structures and compressibilities of pyrope and grossular to 60 kbar, *Amer. Mineral., 63,* 297–303, 1978*b*.

Hazen, R. M., and L. W. Finger, The crystal structures and compressibilities of layer minerals at high pressure, *Amer. Mineral., 63,* 289–296, 1978*c*.

Hazen, R. M., and L. W. Finger, Linear compressibilities of $NaNO_2$ and $NaNO_3$, *J. Appl. Phys., 50,* in press, 1979*a*.

Hazen, R. M., and L. W. Finger, Studies in high-pressure crystallography, *Carnegie Inst. Wash. Yearb., 78,* in press, 1979*b*.

Hazen, R. M., and L. W. Finger, Crystal structure and compressibility of zircon at high pressure, *Amer. Mineral., 64,* 196–201, 1979*c*.

Hazen, R. M., and C. T. Prewitt, Effects of temperature and pressure on interatomic distances in oxygen-based minerals, *Amer. Mineral., 62,* 309–315, 1977*a*.

Hazen, R. M., and C. T. Prewitt, Linear compressibilities of low albite: High-pressure structural implications, *Amer. Mineral., 62,* 554–558, 1977*b*.

Hazen, R. M., L. W. Finger, and T. Yagi, Crystal structure and compressibility of MnF_2 to 15 kbar, *Carnegie Inst. Wash. Yearb., 77,* 841–842, 1978.

Jorgensen, J. D., Compression mechanisms in α-quartz structures—SiO_2 and GeO_2, *J. Appl. Phys., 49,* 5473–5478, 1978.

Liu, L.-G., and W. A. Bassett, Effect of pressure on the crystal structure and the lattice parameters of BaO, *J. Geophys. Res., 77,* 4934–4937, 1972.

Liu, L.-G., and W. A. Bassett, Changes of the crystal structure and the lattice parameter of SrO at high pressure, *J. Geophys. Res., 78,* 8470–8473, 1973.

Lynch, R. W., and H. G. Drickamer, Effects of high pressure on the lattice parameters of diamond, graphite, and hexagonal boron nitride, *J. Chem. Phys., 44,* 181–184, 1966.

Sato, Y., and S. Akimoto, Hydrostatic compression of four corun-

dum-type compounds: α-Al_2O_3, V_2O_3, Cr_2O_3, and α-Fe_2O_3, *J. Appl. Phys., 50,* 5285–5291, 1979.
Schreiber, E., and O. L. Anderson, Pressure derivatives of the sound velocity of polycrystalline alumina, *J. Amer. Ceram. Soc., 49,* 184–190, 1966.
Simmons, G., and H. Wang, *Single Crystal Elastic Constants,* MIT Press, Cambridge, Mass., 1971.
Yagi, T., Experimental determination of thermal expansivity of several alkali halides at high pressure, *J. Phys. Chem. Solids, 39,* 563–571, 1978.

(Received December 21, 1978;
revised June 12, 1979;
accepted July 13, 1979.)